2011 American Control Conference
on O'Farrell Street, San Francisco, CA, USA
June 29 - July 01, 2011

Model-Based Estimation of Ethanol Content in Flexible Fuel Vehicles

Rohit Zope, Matthew Franchek, Karolos Grigoriadis, Gopichandra Surnilla and Stephen Smith

Abstract— **Presented in this paper is a model-based method for accurately estimating the percent ethanol content of an ethanol-gasoline fuel blend used in flexible fuel vehicles (FFVs). Few methods exist in literature addressing the problem of ethanol estimation in production FFVs. The proposed approach has a distinct advantage as it uses the existing sensor set on a production vehicle. Measurements from the sensors are used to adapt a steady state parametric model relating the engine speed, throttle angle opening and the air-fuel ratio to the fuel injector pulse width command. A first-principles physics-based approach is used to develop the model structure. The fuel composition information is embedded in the adapted model coefficients whose variation is used for ethanol content estimation. The method is validated with experiments on a 2005 Ford 5.4-L V8 port fuel injected engine.**

I. INTRODUCTION

Ethanol is a renewable fuel with a potentially neutral CO_2 cycle and is widely used as an alternative to gasoline. Because of the excellent miscibility of ethanol with common gasoline, it can be used as an additive to partially replace the gasoline content of automotive fuel. Such mixtures are normally named after the amount or percentage of ethanol contained in the fuel blend. For example, a mixture containing 85% ethanol and 15% gasoline by volume is referred to as E85. In the United States, E85 is used as an alternative to gasoline and more recently mid-blends such as E20, E30, E50 are made available at select locations. Flexible Fuel Vehicles (FFVs) can operate on any blend of ethanol-gasoline. Such FFVs require changes in the engine management system to meet the emission requirements without sacrificing drivability while exploiting the beneficial fuel properties associated with ethanol. The chemical as well as physical properties of ethanol differ from those of gasoline as shown in Table I. The effect of ethanol fuel on spark ignition (SI) engine is documented in [1]. As can be observed, ethanol has a higher octane rating than gasoline allowing higher compression ratio and higher combustion efficiency without leading to engine knocking. To exploit the fuel properties of ethanol, to improve fuel economy and to maintain engine performance, it is necessary to accurately know the ethanol content in the fuel blend. Capacitance based sensors, could be used to differentiate the fuel blends based on the dielectric constant [2]. However, such sensors have associated reliability and cost issues. Ethanol content estimation can be realized by attributing the output of the feedback fuel regulating control loop after a refill event to the change in ethanol blend fuel. This exhaust gas oxygen (EGO) sensor approach to ethanol estimation is cost effective but becomes less robust in-case of mass air flow sensor errors. This emphasizes the need of an alternative approach to ethanol estimation.

TABLE I
PROPERTIES OF GASOLINE AND ETHANOL [1], [2]

Property	Gasoline	Ethanol
Chemical formula	$C_4 - C_{12}$	C_2H_5OH
Lower heating value (MJ/kg)	42.4	26.8
Density (kg/m^3)	745	790
Research Octane Number	92	111
Stoichiometric air-fuel ratio	14.6	9.0
Dielectric constant	2	24.3
Latent heat of vaporization (kJ/kg)	420	845
Boiling point (°C)	20-300	78.5

Presented in [3] are the engineering challenges of estimating ethanol content on a sensorless system subject to real world issues. One model-oriented approach appeared in [2]. Investigated in this work are the sensitivity issues of ethanol content estimation to errors in air charge, mass air flow (MAF) sensor, and manifold temperature sensor. The conclusion points out the high sensitivity of ethanol estimation and motivates the need of redundant algorithms with fusion of other sensors. The authors in [4] propose the use of a manifold absolute pressure (MAP) sensor along with the MAF sensor to estimate cylinder air flow under MAF sensor drifts and hence prevent severe misestimation of ethanol content in flex fuel vehicles. The effect of fuel ethanol concentration on cylinder pressure evolution in direct-injection flex-fuel engines has been studied in [5] and the use of an in-cylinder pressure sensor proposed in [6]. The methodology in [6],[7] is based on in-cylinder pressure measurements during the compression stroke and exploits the different charge cooling properties of ethanol and gasoline. All the approaches reviewed involve addition of an otherwise redundant sensor, increasing production costs. In this paper, a parametric adaptive model-based approach to ethanol estimation is proposed. A model relating the fueling command to the engine speed and throttle angle is developed. Adaptation in the model coefficients are used to estimate the fuel composition of the fuel blend being used. Experimental results are presented to validate the proposed approach.

II. MOTIVATION

Detailed in this section is the motivation for the approach presented in this work. A steady state fuel path model structure is identified and used in the ethanol estimation process.

Zope. R.A., Franchek. M.A., and Grigoriadis. K.M., are with the Department of Mechanical Engineering, University of Houston, Houston, TX, USA razope@uh.edu

Surnilla. G., and Smith. S., are with the PT Controls Research & Advanced Engineering, Ford Motor Company, Dearborn, MI, USA

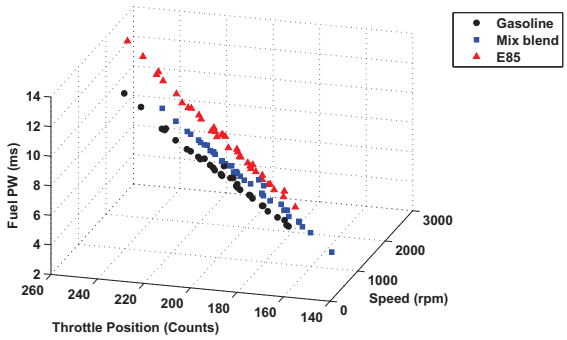

Fig. 1. Fuel PW, Engine Speed and Throttle Position For Three Fuel Types Tested in a 2005 Ford 5.4L Port Injected Engine

Identifying a low order, yet high-fidelity model structure is of utmost importance, as the accurate estimation of ethanol content is based on the identified fuel path model. The ethanol estimation strategy utilizes the observed change in model parameter coefficients to predict the fuel composition.

A. Model Structure Identification

A comparison of the fuel properties for ethanol and gasoline shows a significant change in the stoichiometric ratio of combustion. For the same amount of air mass flow, 48.97% more by mass of ethanol, is required as compared to gasoline to achieve stoichiometry. As the modern day automobiles use a linear exhaust gas oxygen sensor in the fueling control, it is reasonable to assume that λ is maintained close to unity, with excursions happening only during transients or as a result of catalyst modulation. This implies that the fuel mass flow in an SI engine relates linearly to the air mass flow and the fuel composition. The engine used in this investigation was equipped with a MAF sensor that measures the air flow across the throttle plate. However, MAF sensors are prone to aging and drift errors [4]. To overcome this problem, the MAF sensor was eliminated and the air-flow was characterized by the throttle angle and engine speed. The fuel injector pulse width is chosen as an output. Fig. 1 shows the fuel pulse-width (PW) plotted as a function of throttle position counts and the engine speed for three different fuel compositions. It can be seen in Fig. 1, that fuel PW is a good indicator of the fuel composition, for similar operating conditions of the engine. This sets the foundation of this work. To summarize our objective, we seek a steady state model of the following form

$$PW_c = f(\theta^i, N^j, \lambda_s^k) \tag{1}$$

where PW_c is the fuel pulse-width command, θ is the throttle angle, N the engine speed and λ_s is the universal exhaust gas oxygen (UEGO) sensor measured normalized air-fuel ratio. In (1), f is a polynomial function in the variables θ, N and λ. The powers $i, j, k \in Z$ and λ is included in the required model structure to account for any non-stoichiometric operation of the engine, as dictated by the catalyst modulation controller.

III. FIRST PRINCIPLES BASED MODEL

In this section, a physics-based approach is used to develop the model structure relating engine speed, throttle position and air-fuel ratio to fuel pulse width command under steady state conditions. To this end, a mean value model of an SI engine is derived and simplified to a low order polynomial-type model.

A. Air Path Dynamics

The air induction system consists of a throttle body, intake manifold and intake valves. Mathematical models for the air path of an internal combustion engine are well established in the literature and can be explained by the intake manifold filling and emptying dynamics [8]. The dynamics governing the intake manifold pressure is obtained by differentiating the ideal gas law

$$P_m V_m = mRT_m \tag{2}$$

where P_m,V_m,T_m and m denote the pressure in the intake manifold, volume of the intake manifold, temperature and mass of the air in the intake manifold respectively. R is the gas constant. Differentiating (2) gives

$$\dot{P_m} = \frac{RT_m}{V_m}\dot{m} + \frac{mR}{V_m}\dot{T_m} \tag{3}$$

The $\dot{T_m}$ term contributes little to the manifold dynamics and can be neglected [9]. The net mass flow rate of air into the intake manifold is the difference of the mass air flow past the throttle, $\dot{m_{a,th}}$ and the air flow into the cylinders, $\dot{m_{a,cyl}}$. The throttle mass air flow rate, $\dot{m_{a,th}}$ can be modeled using the standard orifice equations for one-dimensional steady compressible flow [8].

$$\dot{m_{a,th}} = C_d A_{th}(\theta) \frac{P_a}{\sqrt{RT_a}} \Psi\left(\frac{P_m}{P_a}\right) \tag{4}$$

where θ is the throttle angle, $A_{th}(\theta)$ is the flow area of the throttle, C_d is the flow discharge coefficient and P_a,T_a denote the ambient pressure and temperature respectively. The functions $A_{th}(\theta)$ and $\Psi\left(\frac{P_m}{P_a}\right)$ are given by

$$A_{th}(\theta) = \frac{\pi {d_{th}}^2}{4}(1 - \cos\theta) \tag{5}$$

where d_{th} represents the throttle plate diameter

$$\Psi\left(\frac{P_m}{P_a}\right) = \begin{cases} \sqrt{\frac{2\gamma}{\gamma-1}\left(r_p^{\frac{2}{\gamma}} - r_p^{\frac{\gamma+1}{\gamma}}\right)}, & \text{if } r_p > \left(\frac{2}{\gamma+1}\right)^{\frac{\gamma}{\gamma-1}} \\ \gamma^{\frac{1}{2}}\left(\frac{2}{\gamma+1}\right)^{\frac{\gamma+1}{2(\gamma-1)}}, & \text{if } r_p \leq \left(\frac{2}{\gamma+1}\right)^{\frac{\gamma}{\gamma-1}} \end{cases} \tag{6}$$

The constant $\gamma = 1.4$ is the ratio of specific heats for air, and $r_p = \frac{P_m}{P_a}$. For online ethanol content estimation, a polynomial approximation to the non-linear equation in

(4) is sought. Equation (5) can be written as a Taylor series expansion leading to

$$A_{th}(\theta) = \frac{\pi {d_{th}}^2}{4}(1-1+\frac{\theta^2}{2!}-\frac{\theta^4}{4!}+\cdots) \quad (7)$$
$$\approx a_0\theta^2 + a_1\theta^4 \quad (8)$$

for some coefficients a_0 and a_1. In this study, the engine was operated at throttle angles resulting in un-choked air flow past the throttle. In a naturally aspirated, engine $P_m < P_a$ except at wide open throttle conditions, when $P_m \rightarrow P_a$. Under these assumptions, the expression for the function $\Psi\left(\frac{P_m}{P_a}\right)$ can be expanded using the generalized binomial theorem as

$$\Psi\left(\frac{P_m}{P_a}\right) = \sqrt{\frac{2\gamma}{\gamma-1}}\left(\frac{P_m}{P_a}\right)^{\frac{1}{\gamma}}\left[1-\left(\frac{P_m}{P_a}\right)^{\frac{\gamma-1}{\gamma}}\right]^{\frac{1}{2}}$$
$$= \sqrt{\frac{2\gamma}{\gamma-1}}\left[\left(\frac{P_m}{P_a}\right)^{\frac{1}{\gamma}} - \frac{1}{2}\left(\frac{P_m}{P_a}\right) + \frac{1}{8}\left(\frac{P_m}{P_a}\right)^{\frac{2\gamma-1}{\gamma}}\cdots\right]$$
$$\approx b_0 P_m^{\frac{1}{\gamma}} + b_1 P_m + b_2 P_m^{\frac{2\gamma-1}{\gamma}} \quad (9)$$

for some coefficients b_0, b_1 and b_2. Substituting the value of γ in (9) results in

$$\Psi\left(\frac{P_m}{P_a}\right) \approx b_0 P_m^{\frac{5}{7}} + b_1 P_m + b_2 P_m^{\frac{9}{7}} \quad (10)$$

Substituting the expressions (8) and (10) into (4) leads to a polynomial expression for the mass of air flow past the throttle plate as given by (11)

$$\dot{m_{a,th}} \approx C_d \frac{P_a}{\sqrt{RT_a}}(a_0\theta^2 + a_1\theta^4)(b_0 P_m^{\frac{5}{7}} + b_1 P_m + b_2 P_m^{\frac{9}{7}}) \quad (11)$$

The coefficient of discharge, C_d is a function of the throttle angle. However, this effect can be incorporated in the a_i coefficients and hence no separate polynomial dependence is considered. This leads to the following polynomial expression for $\dot{m_{a,th}}$

$$\dot{m_{a,th}} \approx c_0\theta^2 P_m^{\frac{5}{7}} + c_1\theta^2 P_m + c_2\theta^2 P_m^{\frac{9}{7}} + c_3\theta^4 P_m^{\frac{5}{7}} + c_4\theta^4 P_m + c_5\theta^4 P_m^{\frac{9}{7}} \quad (12)$$

for some coefficients c_i. This completes the approximation of the mass air flow past the throttle plate in a polynomial form.

The mass of air inducted into the cylinders is modeled by considering the engine to be a volumetric pump as is standard in the literature [8] [10]. The cylinder air flow for a 4-stroke engine is given by

$$\dot{m_{a,cyl}} = \frac{\eta_{vol}\rho_{a,m}V_d N}{2} \quad (13)$$

where η_{vol} is the volumetric efficiency, $\rho_{a,m}$ is the density of air in the intake manifold and V_d is the total displaced volume of all the cylinders. Using the ideal gas law equation (2), (13) can be written as

$$\dot{m_{a,cyl}} = \frac{\eta_{vol}V_d N}{2RT_m}P_m \quad (14)$$

As is a common practice [11] [12], the volumetric efficiency is expressed as a polynomial function of P_m and N.

$$\eta_{vol} = d_0 + d_1 N + d_2 N^2 + d_3 N^2 + d_4 P_m \quad (15)$$

Substituting (15) in (14) gives

$$\dot{m_{a,cyl}} \approx e_0 N P_m + e_1 N^2 P_m + e_2 N^3 P_m + e_3 N P_m^2 \quad (16)$$

Under steady state operation, (3) gives $\dot{m_{a,th}} = \dot{m_{a,cyl}}$. Equating (12) and (16) permits a solution to the air flow rate into the cylinders using only engine speed, N and the throttle angle, θ. The variable P_m is thus eliminated. This however leads to a complicated expression involving non-integer powers of P_m. To further simplify, consider the terms with only the integer powers of P_m in (12) as

$$\dot{m_{a,th}} \approx c_1\theta^2 P_m + c_5\theta^4 P_m \quad (17)$$

Solving for P_m from (17) and (16) and substituting back in (17) gives an expression for the mass flow rate of air into the cylinders, MAF_{cyl} as

$$MAF_{cyl} = \frac{c_1\theta^2}{e_3}\left(-e_0 - e_1 N - e_2 N^2 + c_1\frac{\theta^2}{N}\right) + \frac{c_5\theta^4}{e_3}\left(-e_0 - e_1 N - e_2 N^2 + c_1\frac{\theta^2}{N}\right)$$
$$\approx f_0\theta^2 + f_1\theta^2 N \quad (18)$$

where in the approximation only the first few significant terms are considered, and f_0, f_1 are some model coefficients. Equation (18) needs to be divided by the engine speed to convert the mass air rate from g/sec to g/cycle or g/intake-event. This is necessary as the steady state model relates the fuel pulse width commanded by the PCM to the air flow per cycle. Hence, the mass air flow rate into the cylinders per intake event is given as a function of throttle angle and engine speed as follows

$$MAF_{cyl/intake} = f_0\frac{\theta^2}{N} + f_1\theta^2 \quad (19)$$

B. Fuel Path Dynamics

Fuel path dynamics have been studied extensively in the past, see [11] [13] and the references there-in. For a port fuel injected system, the fuel puddling phenomenon is used to explain the dynamics relating the injected fuel mass to the fuel mass actually entering the cylinders. Under steady state operation of the engine, the fuel mass in the cylinder would equal the injector's command. The fuel system is usually designed such that the fuel flow rate is proportional to the injection pulse width command as given by

$$PW_c = K_{fpw}\dot{m_{f,c}} \quad (20)$$

where PW_c is the injection pulse width command, K_{fpw} is a constant characterizing the fuel injector's slope and $\dot{m_{fc}}$

is the fuel command from the PCM. As explained above the actual fuel mass flow in the cylinders has the same value as the fuel commanded, giving the equation

$$\dot{m_{f,cyl}} = \dot{m_{f,c}} \tag{21}$$

C. UEGO Sensor Dynamics

The UEGO sensor is used to measure the air-fuel ratio in the exhaust gas of an SI engine. More specifically the UEGO sensor located in the exhaust manifold reads the normalized air-fuel ratio, λ which is defined as

$$\lambda = \frac{\dot{m}_a/\dot{m}_f}{AFR_{stoic}} \tag{22}$$

where AFR_{stoic} is the mass ratio of air-fuel for stoichiometric combustion. Associated with the UEGO sensor dynamics is a time delay and a first order lag. The delay is a result of the transport of exhaust gas species from the cylinders' exhaust port downstream to the location of the UEGO sensor. The first order lag captures the dynamics associated with the gas mixing, as well as the sensor response. In the frequency domain, this results in the following expression for the sensed value of the normalized air-fuel ratio, λ_s

$$\lambda_s(s) = e^{-Ts}\frac{1}{\tau s + 1}\lambda_{cyl}(s) \tag{23}$$

where T, τ denote the time delay and the time constant respectively. Thus λ_{cyl} is the engine operating air-fuel ratio given as

$$\lambda_{cyl} = \frac{MAF_{cyl/intake}/\dot{m_{f,cyl}}}{AFR_{stoic}} \tag{24}$$

λ_s denotes the normalized air-fuel ratio reading from the UEGO sensor, that would equal λ_{cyl} when the engine is operating at steady state. Substituting (19), (20) and (21) in (24) results in a steady state model for the fuel injection pulse width command

$$PW_c = \frac{K_{fpw}}{\lambda_s AFR_{stoic}}\left(f_0\frac{\theta^2}{N} + f_1\theta^2\right) \tag{25}$$

As a final outcome the following modification of (25) is proposed

$$PW_c = \alpha_0\theta^2 + \alpha_1\left(\frac{\theta^2}{N}\right) + \alpha_2\left(\frac{1}{\lambda_s}\right) \tag{26}$$

The advantage of (26) over (25) is that the number of regressor multiplications are reduced. This form relates sensor faults to specific coefficient(s) within the model and from this isolation sensor diagnostics can be performed. Combining the sensor diagnostics component of (26) along with its ethanol estimation capability enables the estimation robustness.

IV. DESCRIPTION OF THE EXPERIMENTAL FACILITY

This study was undertaken at the University of Houston's Engine Control Research facility. The engine used is a 2005 Ford 5.4-L V8 sequential multi-port fuel injected, spark ignition engine, controlled by a Ford production Powertrain Control Module (PCM). The interface to this PCM is provided by a memory emulator. The engine is equipped with a variety of production sensors. The sensors of interest are the throttle position sensor, crankshaft position sensor and the UEGO sensor. The software used for data acquisition and control was by Accurate Technologies. The software runs on a Dell computer which communicates with the memory emulator via the USB port. The software has two components called the "ATI VISION" and the "ATI No-Hooks". The ATI VISION allows for the monitoring and measurement of signals that the PCM broadcasts, whereas the ATI No-Hooks allows access to RAM variables internal to the PCM, which are otherwise only viewable or measurable. The engine is coupled to a 175-hp eddy current dynamometer. The dynamometer is controlled by a DyneSystems InterLoc-V controller. To achieve steady state at different operating conditions, the throttle plate was controlled using the No-Hooks software, whereas the torque load on the engine was controlled using the dynamometer controller. Fuel injectors were left in control of the Ford PCM.

TABLE II
EXPERIMENTAL DATA OBTAINED MODEL COEFFICIENT

	E10	E40	E70	E85
α_0 coefficient	1.28	1.50	1.66	1.76
α_1 coefficient	2.27	2.49	2.784	3.2
α_2 coefficient	-5.17	-6.0	-6.443	-7.34
Total Squared Error	0.21	0.6	0.56	0.69
Length of Vector	5.8	6.67	7.213	8.23

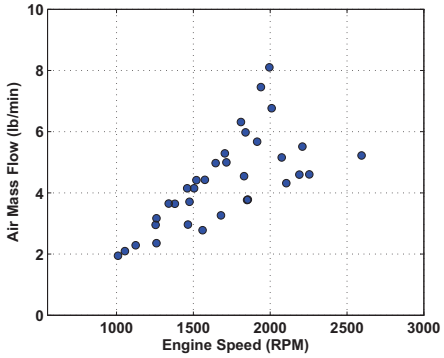

Fig. 2. Air Mass Flow - Engine Speed Operating Points

V. RESULTS AND DISCUSSION

Presented in this section are the results of using experimental data to identify model coefficients for the model structure in (26). Based on the identified coefficients, an ethanol content estimation methodology is proposed and validated.

A. Experimental Validation of the Model

Equation (26) defines the model to be adapted for ethanol estimation. E10, E40, E70 and E85 are the four fuel blends used to perform test runs and collect data in this study. With a

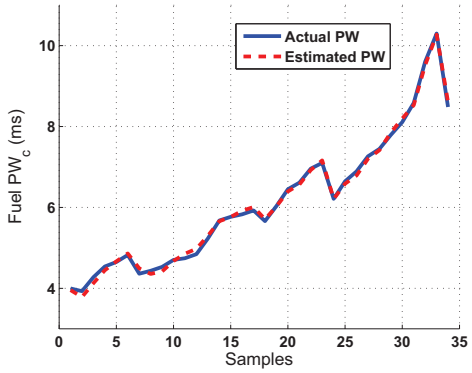

Fig. 3. Actual V/s Modeled PW$_c$ for E10 Fuel

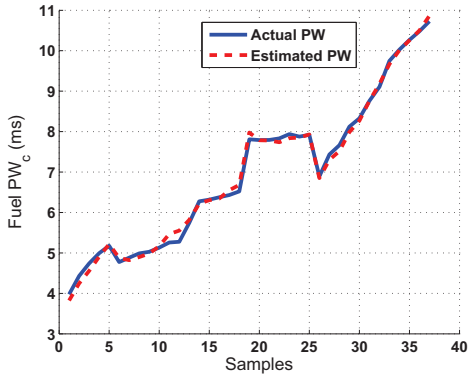

Fig. 4. Actual V/s Modeled PW$_c$ for E40 Fuel

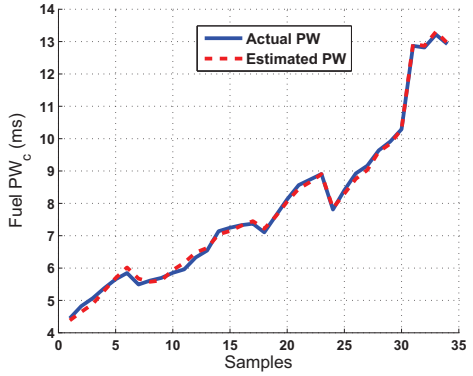

Fig. 5. Actual V/s Modeled PW$_c$ for E70 Fuel

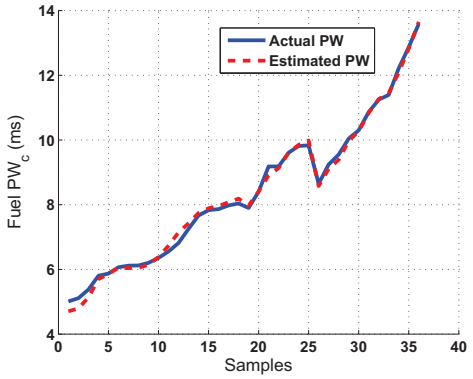

Fig. 6. Actual V/s Modeled PW$_c$ for E85 Fuel

known fuel composition in the tank, the engine was operated over the speed-load points shown in Fig. 2. At each steady state, the engine speed was controlled using the throttle, load was controlled using the dynamometer and all the relevant data recorded using the ATI-VISION recorder software. The data was post-processed and the α-coefficients identified using a Recursive Least Squares(RLS) method. The values of the α-coefficients obtained are as shown in Table II. Fig. (3) shows a comparison of the model estimated fuel PW$_c$ with the actual PCM commanded fuel PW for the E10 fuel blend. Figures (4), (5) and (6) show the same comparison for the E40, E70 and E85 fuel blends respectively. As is evident from the figures, the proposed model has estimated the PCM commanded PW, very closely. The associated squared errors for the estimates are shown in Table II.

B. Ethanol Content Estimation Methodology

In Section III, a physics-based model relating the throttle angle, engine speed and lambda sensor output to fuel PW was developed. The model structure was validated using experimental data in the preceding subsection. This section presents the method used to estimate percent ethanol based on the adapted model coefficient values. As the model coefficients depend on the stoichiometric ratio of combustion associated with the fuel, the coefficient values would vary with the change in fuel composition. This change can be linked to the content of ethanol present in the fuel blend. The three coefficients α_0, α_1 and α_2 define a vector in $\mathbf{R}^3$. The length of this vector changes with changing fuel composition and is a metric indicating the ethanol content in the blend. A 3-dimensional plot of the vectors can be obtained; However for the sake of clarity we have shown in Fig. 7 the projection of the vectors in the α_1, α_2 plane. As is evident the vectors lengths vary with fuel composition.

This observation is further justified by considering the ratio of the lengths of the vectors, for the E85 and E10 fuel. Equation (25) states that the model coefficients should relate inversely to the stoichiometric ratio of the fuel-blend. Hence, we have, as the expected ratio of the vector lengths

$$\frac{L_{E85,expected}}{L_{E10,expected}} = \frac{AFR_{stoic,E10}}{AFR_{stoic,E85}} = \frac{14.01}{9.8} = 1.42 \qquad (27)$$

Table II gives the value of this ratio for the actual lengths as

$$\frac{L_{E85,actual}}{L_{E10,actual}} = \frac{8.23}{5.8} = 1.418 \qquad (28)$$

As can be observed from (27) and (28) the observed value and the expected value are close enough and the introduced error is less than 0.15%. Table III gives the expected and

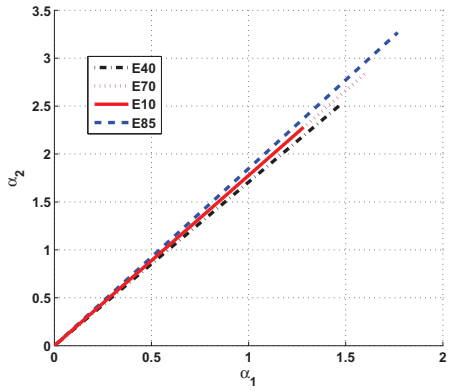

Fig. 7. Vectors projected in the $\alpha_1 - \alpha_2$ plane

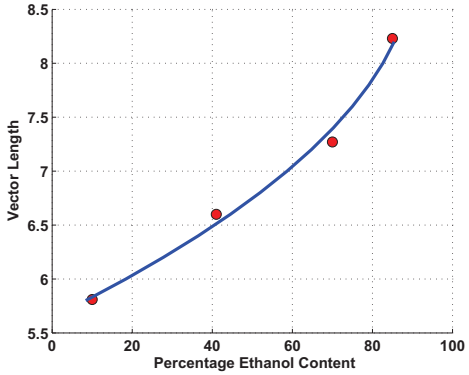

Fig. 8. Vector Length V/s Percent Ethanol Content

observed vector length ratios for the four fuel blends tested. Table III further asserts the claim that the vector length changes with fuel composition. Figure 8 shows a plot of the vector lengths as a function of percent ethanol, by fitting a curve through the four points obtained from experiments. This relationship can be used to estimate the percent ethanol content in a fuel blend, by adapting the model coefficients of (26) online.

VI. Conclusion and Future Work

In this paper, a method for online estimation of ethanol content in flex-fuel vehicles using the existing sensor set is presented. Throttle position measurement along with engine speed, gives an estimate of the air-flow rate in the cylinders. Use of throttle position sensor as opposed to the MAF sensor, eliminates any sensitivity issues associated with the MAF sensor. A steady state model of the fueling command is developed using a first-principles based approach. The model coefficients are shown to capture the effect of changing fuel composition. Adaptation in the model coefficients is used to estimate accurately the ethanol content. The proposed approach has been validated experimentally, by collecting data at the University of Houston's Engine Control and Research Laboratory.

TABLE III
Expected and Observed Vector Length Ratios

	Expected Ratio	Observed Ratio
$\frac{L_{E10}}{L_{E10}}$	1	1
$\frac{L_{E40}}{L_{E10}}$	1.14	1.148
$\frac{L_{E70}}{L_{E10}}$	1.31	1.243
$\frac{L_{E85}}{L_{E10}}$	1.42	1.418

This work has focussed on providing a proof of concept, relating the parameter vector length to fuel composition. This idea can be extended further by looking at the direction of the vectors, along with the length to provide a diagnostic capability, in-case of any sensor measurement inaccuracies.

VII. Acknowledgments

This material is based upon work supported by the National Science Foundation under Grant No. 0727999. Any opinions, findings and conclusions or recommendations expressed in this material are those of the author(s) and do not necessarily reflect the views of the National Science Foundation. The authors also gratefully acknowledge the support of Ford Motor Company.

References

[1] Nakata, K., Utsumi, S., Ota, A., Kawatake, K., Kawai, T., and Tsunooka, T., "The effect of ethanol fuel on a spark ignition engine", *SAE Paper 2006-01-3380*

[2] Ahn K., Stefanopoulou A.G. and Jankovic M., "Estimation of ethanol content in flex-fuel vehicles using an Exhaust Gas Oxygen sensor: model, tuning and sensitivity", *In Proceedings of the ASME 2008 Dynamic Systems and Control Conference*, DSCC2008-12345, 2008, pp 1-7

[3] Theunissen, F.M.M., "Percent ethanol estimation on sensorless multi fuel systems; advantages and limitations", *SAE Paper 2003-01-3562*

[4] Ahn K., Stefanopoulou A.G. and Jankovic M., "Tolerant ethanol estimation in flex-fuel vehicles during MAF sensor drifts", *In Proceedings of the ASME 2009 Dynamic Systems and Control Conference*, DSCC2009-2708, 2009, pp 1-8

[5] Oliverio, N.H., Jiang L., Yilmaz H., and Stefanopoulou, A., "Modeling the effect of fuel ethanol concentration on cylinder pressure evolution in direct-injection flex-fuel engines", *In Proceedings of the 2009 American Control Conference*, June 2009, pp 2307-2044

[6] Oliverio, N.H., Jiang L., Yilmaz H., and Stefanopoulou, A., "Ethanol detection in flex-fuel direct injection engines using in-cylinder pressure measurements", *SAE Paper 2009-01-0657*

[7] Ahn, K., Stefanopoulou, A., Jiang, L., and Yilmaz, H., "Ethanol content estimation in flex fuel direct injection engines using in-cylinder pressure measurements", *SAE Paper 2010-01-0166*

[8] Heywood, J., "Internal combustion engine fundamentals", New York, NY, USA:McGraw-Hill

[9] Hendricks, E., Chevalier, M.J., Sorensen, S.C., Trumpy, D., and Asik, J., "Modeling of the Intake Manifold Filling Dynamics", *SAE Paper 960037, 1996*

[10] Powell, B.K., "A Dynamic Model for Automotive Engine Control Analysis", *In Proceedings of the 18th IEEE Conference on Decision and Control including the Symposium on Adaptive Processes*, 1979, pp 120-126

[11] Franchek, M.A., Mohrfield, J., and Osburn, A., "Transient Fueling Controller Identification for Spark Ignition Engines", *Journal of Dynamic Systems and Control* , June 2006, Vol.1, Issue 3, pp 449-460

[12] Guzzella, L., and Onder, C.H., "Introduction to Modeling and Control of Internal Combustion Engine Systems", 2004, Springer

[13] Aquino, C.F., "Transient A/F Control Characteristics of the 5 Liter Central Fuel Injection Engine", 1981, *SAE Technical Paper No. 810494*